VOL. 18, NO. 20, OCTOBER 2023 ISSN 1819-6608
ARPN Journal of Engineering and Applied Sciences

www.arpnjournals.com

UTILIZING INNOVATIVE NANOLIME-GEOPOLYMER AS A CEMENT FOR GAS WELLS

Mario E. S. Abdelmalek, Said K. E. Salem, Mahmoud A. Tantawy and Shady G. El Rammah
Department of Petroleum Engineering, Faculty of Petroleum and Mining Engineering, Suez University, Egypt
E-Mail: marioemad64@gmail.com

ABSTRACT

This paper is to introduce the formulation of the innovative nanolime-geopolymer NLGP and its application in gas wells as a replacement for the traditional cement. The new mix is composed of nanolime NL, fly ash, sodium hydroxide, and sodium silicate. The compressive strengths of NLGP are measured using different molarities, and ratios of its components to compare and evaluate the results. After that, a detailed profit study in USD will show the profitability of NLGP compared to other types of current cement and the possibility of its manufacturing. Also, a separate comparison to cement fly ash CF was done. Finally, the "deep water horizon" incident will be used as a case study to indicate the applicability of NLGP in such cases for stopping gas channeling which occurs due to cement job failure.

Keywords: nano-cement, gas wells, cementing, geopolymer, deep water horizon.

Manuscript Received 24 September 2023; Revised 22 November 2023; Published 30 December 2023

1. INTRODUCTION AND LITERATURE REVIEW

Nanoparticles (NPs) technology has wide and modern applications in the field of petroleum engineering because of the higher area to volume ratio which establishes a stronger and light weight product. To obtain the high weight requirements, nanofluid is designed by mixing NPs with a solvent. The reference of nano size is between 1 and 100 nm.

This research paper is an experimental work to introduce nanolime's (NL) effect on geopolymer. Before moving to the methodology of preparing nanolime-geopolymer (NLGP) experimentally and testing the resulting material, the following literature review is to introduce the previous work and show the need for NLGP.

All the literature review works are chosen to show the developing stages of nanotechnology and the importance of geopolymer economically and environmentally. The methodology work will get the advantage of all the literature review work by showing the effect of applying nanotechnology on geopolymer. Therefore, the final product will be "nanolime-geopolymer" (NLGP). The final results have to show the high value compressive strength of the product which is a summation of all the literature review works. NLGP design has to consider exposure to gas instead of oil.

Literature review starts with the application of nanotechnology in petroleum engineering. Nanoparticles' applications extend to drilling, completion, production, and enhanced oil recovery. They are used in the drilling fluid to plug the formation's pores to control drilling mud invasion into fresh water zones. Also, pores plugging is targeted in order to reduce shale swelling. The high area to volume ratio of NPs means that the area of exposure is high which makes it more suitable for drilling reactive, pliable, tenacious shale. Such shale types would cause bit balling and reduce the rate of penetration. In completion, NPs are used in the hydraulic fracturing fluid to control the gel breaking time after the end of the hydraulic fracturing job. In addition, they help in a better distribution of the proppant, which in turn, leads to higher production. To increase production efficiency, nanotechnology is used in two ways. The first way is the protective way in which the reservoir is less damaged by the nano-based drilling fluid. The second way is the use of NPs in the polymer fluid as an enhanced oil recovery technique. Therefore, the resulting areal sweep efficiency of nanopolymer fluid increases, and residual oil saturation decreases.

In 2012, when Roige *et al*, added nano calcium silicates to cement, they found a significant change in the cement hydration process. The structure of the produced cement was crystalline (like ductile fiber), which in turn minimized capillary pores. Therefore, the risk of micro cracking and oil seepages was reduced.

In 2016, Chimaroke *et al*, showed experimentally the effect of using NPs in drilling fluid. They recorded a substantial reduction in drilling fluid loss inside test samples which represented the formations. Finally, the calculated value of skin factor was minimal in comparison to the values resulting from normal drilling fluids' invasions. They explained the resulting economic advantages as follows:

In drilling, the lost drilling fluid creates an additional cost, so minimizing losses "by using nano drilling fluids" results in higher profit. In production, if the pay zone was drilled with normal drilling fluid, the fluid contamination would be higher, and less production is expected. In low porosity pay zones, such oil production would be minimal due to oil phase trapping by capillary forces of drilling fluid invasions. Also, an emulsion would be formed by the interaction between the oil and filtrate.

They have chosen the mica and the alumina nanoparticles. The mica was sieved in different sizes. Four samples of drilling fluids were formulated. The samples consisted of: no fluid loss additives (sample#1), 20-235 micron sizes of mica (sample#2), 20-200 micron sizes of mica (sample#3), and alumina NPs (sample#4).

Filter tests showed that sample#4 causes the least volume of filtrate invasion and the least permeable filter cake. Compared to sample#1, the percentages of reduction in fluid loss are: 43.48 % for sample#4, 26.09 % for sample#3, and 13.04 % for sample#2. Consequently, the percentages of reduction in fluid loss from sample#1 to sample#3 are equal, but there is a big gap between sample#3 and sample#4. Therefore, alumina NPs proved the efficiency in reducing the volume of filtrate invasion and the permeability of filter cake.

In China, Geopolymers proved high corrosion and fire resistance properties with the highest compressive strength properties (Lahoti *et al*., 2019), (Aiken *et al*., 2018), (Liu *et al*., 2020c), (Aliques-Granero *et al*., 2019) and (Shill *et al*., 2020). Before the 1990s, geopolymer was widely used because of its high compressive strength and lower permeability. It was used for coating lightweight poly-styrene roofs (Lyu *et al.*, 2019) and (Abdel- Ghani *et al.*, 2019). Wang *et al*. (2016) explained that geopolymer is so useful and needs very low water. Geopolymers were used in military applications to resist explosions and hazardous materials (Shill *et al*., 2020). The use of fly ash as an alkali material to resist acidic materials was shown by (Liu *et al*., 2020b). Using geopolymer helps to reduce the fly ash amount in the atmosphere (which is radio-active) and get a clean environment while using this ash in geopolymer (Dindi *et al*., 2019). In 2017, radio-active materials emissions in China exceeded three million and five hundred thousand tons, and only five percent were utilized (Li *et al* 2018). The collected radio-active materials occupy wide areas of land and cause environmental problems, especially for water and soil (Zhao *et al*., 2020d, Yang *et al*, 2019). In China, garbage gathering was two hundred million tons in 2017, most of which is mainly harmful to soil and water (Zhang *et al*., 2020d). Geopolymer helps in facing such challenges by using such waste material and reducing the consumption of natural resources for cementing purposes.

All the previous literature review works showed that NPs and geopolymer are important to recent industries. But, there was no communication between them. The next methodology will utilize NPs in geopolymers for developing the cementing industry. The results will be used to analyze the enhancements in compressive strength, profitability, and applicability.

2. MATERIAL AND METHODS

2.1 Preparing Nanolime

The process starts with preparing NL using an innovative way. Limestone (purity = 99.3 % for CaCO3) (Figure-1) was heated to eight hundred degrees Celsius which resulted in calcium oxide and carbon di-oxide. Then, calcium hydroxide was obtained by adding 50 cubic centimeters of water to one hundred gm of calcium oxide. After that, calcium hydroxide was dried and ground in a mill (applying the same speed and duration to get 30 microns size).


THE MINISTRY OF PETROLEUM
THE EGYPTIAN MINERAL RESOURCES AUTHORITY
Central Laboratories Sector
1, Ahmed El-Zaiat St, Dokki - Gezah - Egypt
Tel: 33370511 – 33370732
Fax: 33371168

وزارة البترول
الهيئة المصرية العامة للثروة المعدنية
الإدارة المركزية للمعامل
١ ش أحمد الزيات - الدقى

الإدارة العامة للمعامل الكيميائية

الجهة الطالبة للتحليل		رقم الخطاب الوارد	٧٧٤
رقم البعثة		المنطقة	
نوع العينات وعددها	حجر جيري بس – عينة	تاريخ ورود العينات	٢٠١٩/٤/١

الرقم الوارد	بدون	
الرقم المركزي	3571	
SiO_2	0.13	%
Fe_2O_3	0.01	%
CaO	55.88	%
MgO	0.08	%
Na_2O	0.06	%
K_2O	N.D	%
Cl^-	0.07	%
SO_3	N.D	%
$CaCO_3$	99.34	%
L.O.I	43.78	%

ملاحظات : العينة مسئولية العميل ولا تمثل الا نفسها
قام بالتحليل : د / سحر فرحات – م/ سيدة اسماعيل
راجع :
مدير عام
الإدارة العامة للمعامل الكيميائية
مدير الإدارة
صفاء

Figure-1. Chemical analysis of Egyptian limestone.

The resulting size distribution was measured by a dynamic light scattering machine (DLS). The particle size was found to be in nano scale. This product is called nanolime (NL). To test NL's strength in a simple way, two hundreds grams of ground sand were to one hundred grams of NL and 50 cubic centimeters of water in three stages. This formulated simple cement was left for three days between two bricks. The result showed that the formulated cement held the two bricks strongly more than usual (Figure-2).

The same process was repeated till obtaining a dry calcium oxide. That time the process was different because calcium oxide was mixed with sand, and then they were ground simultaneously while applying the previous grinding parameters. This led to the formation of a stronger cement product than the previous one. The reason is that mixing while grinding led to obtaining a smaller NL size and therefore, led to formulating a stronger cement.

Figure-2. NL and sand (simple cement).

Preparing and Testing NLGP

a. Test samples were prepared as per Egy-Code: 203 for the year 2008. All materials were used in micron sizes, Table-1. CEMI N42.5 was used from Suez Company, Table-2. The solution of sodium silicate was purchased from Egypt Silicates Company, table-3. 99% purity sodium hydroxide was obtained from the local market. Fly ash is class F as per ASTM C-618, table-4 and table-5. The particle surface area of fly ash is nearly 2980 cm2/gm, table-6 and table-7. Finally, nanolime was added in 1 %. The chemical analysis of a limestone sample from Egypt (Samalut formation) shows a purity of 99.34% for CaCO3 (Figure-1).

Table 1: Physical properties of fine aggregate

Property	Results	Limits
Specific Weight	2.63	2.5-2.75 **
Bulk Density (t/m3)	1.78	-----
Fineness Modulus	2.89	-----
Clay and Fine Dust Content (% By Volume)	0.85	Not more Than 3% **

** Egyptian Stander Specifications ESS 1106 [16].

Table 2: Physical properties of ordinary Portland cement.

Property		Results	Specifications Limits*
Compressive Strength of Standard Mortar (Mpa)	3 days	21.4	Not less than 18
	28 days	39.7	Not less than 36
Fineness in terms of S.S.A** (cm2/gm)		3185	>2750
Setting Time (min)	Initial	75	Not less than 45
	Final	480	Not more than 600

* Egyptian Stander Specifications ESS 4756-1/2009 [14].

Table 3: Chemical and physical properties of sodium silicate solution

Product Name	Data
SiO2/Na2O ratio	2.00
%Na2O	14.70
%SiO2	29.70
% Total solid	44.40
% Water content	55.55
% Water insoluble	0.05
Baume	50
Specific gravity at (20°C) g/cm3	1.526
Color and appearance	Clear white liquid
PH	12.7

Table (4): Physical properties of the used fly ash

Property	Test Results
Specific surface area (cm^2/gm)	3950
Bulk density (kg/m^3)	1250
Specific gravity	2.5
Color	Light gray

Table (5): XRF Analysis for the used fly ash

Oxide	Content %	Limitation % *
SiO_2	61.30	Min. 70%
Al_2O_3	29.40	
Fe_2O_3	3.27	
CaO	1.21	-----
MgO	0.75	-----
K_2O	1.20	-----
SO_3	0.003	Max. 3%

Table (6): Physical properties of the used cement kiln dust (by-pass).

Property	Test Results
Specific surface area (cm^2/gm)	2980
Bulk density (kg/m^3)	1150
Specific gravity	2.81
color	Light gray
Physical Form	Powder

Table (7): XRF Analysis for the used cement kiln dust (by-pass).

Oxide	Content %
SiO_2	16.65
Al_2O_3	4.48
Fe_2O_3	2.08
CaO	41.87
MgO	2.33
K_2O	5.20
SO_3	2.15
Na_2O	4.16
Cl	3.36
LOI	11.82

Sodium hydroxide (NaOH) was used as the alkaline element which activates the reaction between sodium silicate (NaSi) and fly ash to obtain the required properties of geopolymer. Safety precautions have to be taken into consideration because such materials are harmful to the skin. Gloves, goggles, and masks have to be used during the experiment.

Fly ash (Figure-3) and dry calcium oxide were mixed dry (2-3 mins). Figure-4 shows the mixer and materials. Then, they were ground in a mill (300 rpm for 5 minutes) to help in obtaining a smaller size of Nl. After that, NaOH and NaSi were mixed with them (5-6 mins). After that, water was mixed (3-4 Mins). Followed by, pouring mixtures in 50X50X50 mm cubes (Figure-5). Finally, the cubes were placed inside the oven (60 degrees Celsius) (Figure-6). After two hours, they were taken outside the oven to room temperature before testing (Figure-7). Compressive strength tests were executed on the 3rd, 7th, and 28th days. The tested specimens were confirmed to be at room temperature.

Figure-3. Fly ash ready to be mixed.

Figure-4. Mixer and materials.

Figure-5. Pouring NLGP inside 50x50x50 mm cubes.

Figure-6. Heating NLGP cubes.

Figure-7. NLGP cubes in room temperature (6% and 12% NLGP are marked from right to left respectively).

3. RESULTS AND DISCUSSIONS

3.1 Results of Dynamic Light Scattering for NL

The size distribution of NL was measured by dynamic light scattering machine (DLS). DLS can be referred to Quasi Elastic Light Scattering (QELS) which is a non-invasive, well-established technique for measuring the size distribution in the submicron sizes reaching 1 nm. Typical applications of dynamic light scattering are the characterization of particles, emulsions, or molecules that have been dispersed or dissolved in a liquid. The Brownian motion of particles or molecules in suspension causes laser light to be scattered at different intensities. Analysis of these intensity fluctuations yields the velocity of the Brownian motion and hence the particle size distribution using the Stokes-Einstein relationship (Tables 8, 9, and 10 and Figure-8):

Note that, NL's size distribution was measured before mixing. This is due to adherence to the main objective of this work (Effect of NL). But in industry, grinding of components comes after mixing them. Consequently, the actual NL's size distribution is smaller because the fly ash will be ground with calcium oxide. This was explained in detail, in section 2.1.

Table-8.

Z-Average (nm): 1007.492
Standard Deviation: 0
%Std Deviation: 0
Variance: 0

Size d.nm	Mean Number %	Std Dev Number %	Size d.nm	Mean Number %	Std Dev Number %
0.4000	0.0		5.615	0.0	
0.4632	0.0		6.503	0.0	
0.5365	0.0		7.531	0.0	
0.6213	0.0		8.721	0.0	
0.7195	0.0		10.10	0.0	
0.8332	0.0		11.70	0.0	
0.9649	0.0		13.54	0.0	
1.117	0.0		15.69	0.0	
1.294	0.0		18.17	0.0	
1.499	0.0		21.04	0.0	
1.736	0.0		24.36	0.0	
2.010	0.0		28.21	0.0	
2.328	0.0		32.67	0.0	
2.696	0.0		37.84	0.0	
3.122	0.0		43.82	0.0	
3.615	0.0		50.75	0.0	
4.187	0.0		58.77	0.0	
4.849	0.0		68.06	0.0	

Table-9.

Derived Count Rate (kcps): 13318.9295259...
Standard Deviation: 0
%Std Deviation: 0
Variance: 0

Size d.nm	Mean Number %	Std Dev Number %	Size d.nm	Mean Number %	Std Dev Number %
78.82	0.0		1106	0.1	
91.28	4.4		1281	0.0	
105.7	17.3		1484	0.0	
122.4	27.4		1718	0.0	
141.8	23.3		1990	0.0	
164.2	12.1		2305	0.0	
190.1	4.0		2669	0.0	
220.2	0.6		3091	0.0	
255.0	0.0		3580	0.0	
295.3	0.0		4145	0.0	
342.0	0.1		4801	0.0	
396.1	0.5		5560	0.0	
458.7	1.4		6439	0.0	
531.2	2.2		7456	0.0	
615.1	2.4		8635	0.0	
712.4	2.1		1.000e4	0.0	
825.0	1.4				
955.4	0.6				

Table-10.

Derived Count Rate (kcps): 13318.9295259...
Standard Deviation: 0
%Std Deviation: 0
Variance: 0

Size d.nm	Mean Number %	Std Dev Number %	Size d.nm	Mean Number %	Std Dev Number %
78.82	0.0		1106	0.1	
91.28	4.4		1281	0.0	
105.7	17.3		1484	0.0	
122.4	27.4		1718	0.0	
141.8	23.3		1990	0.0	
164.2	12.1		2305	0.0	
190.1	4.0		2669	0.0	
220.2	0.6		3091	0.0	
255.0	0.0		3580	0.0	
295.3	0.0		4145	0.0	
342.0	0.1		4801	0.0	
396.1	0.5		5560	0.0	
458.7	1.4		6439	0.0	
531.2	2.2		7456	0.0	
615.1	2.4		8635	0.0	
712.4	2.1		1.000e4	0.0	
825.0	1.4				
955.4	0.6				

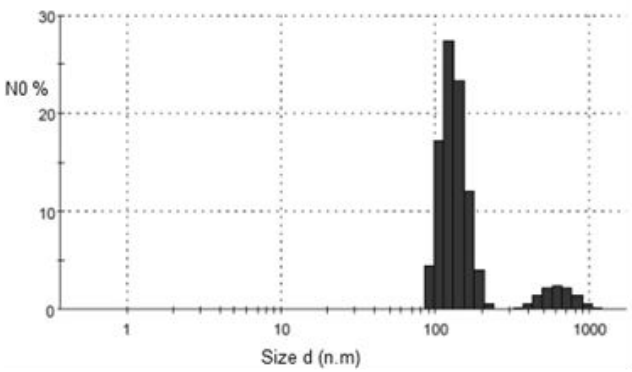

Figure-8. Standard deviation bar.

3.2 Compressive Strength Results

3.2.1 Compressive strength for various molarities and ratios of components

Compressive strength values of NLGP were measured when the ratios between NaOH: NaSi had been 1:1, 1:2, and 1:3 (while the other components were fixed). These values were recorded for three different molarities of NaSi (M10, M14, and M16). The results are shown in Figure-9, Figure-10 and Figure-11 respectively. The obtained compressive strength of the NLGP sample (NaOH:NaSi = 1:1, M16) was more than Portland cement by 24% on the 7th and 29% on the 28th day. In addition, on the 7th day, NLGP recorded a 12% increase in compressive strength more than Portland cement on its 28th day. Finally, all compressive strength values of NLGP were compared to Portland cement on the 3rd, 7th, and 28th day.

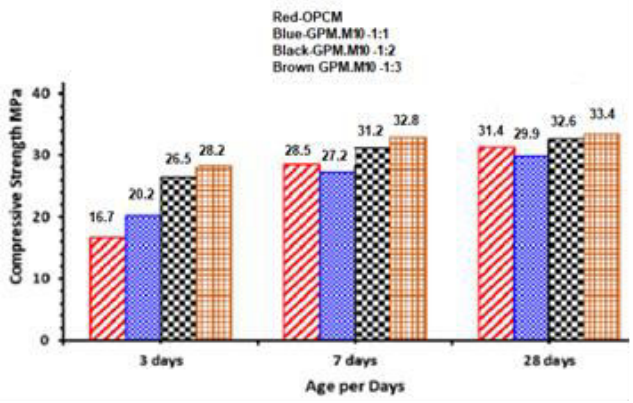

Figure-9. Effect of sodium silicate solution-to-sodium hydroxide solution with molarity M10 on compressive strength (for days: 3, 7 and 28).

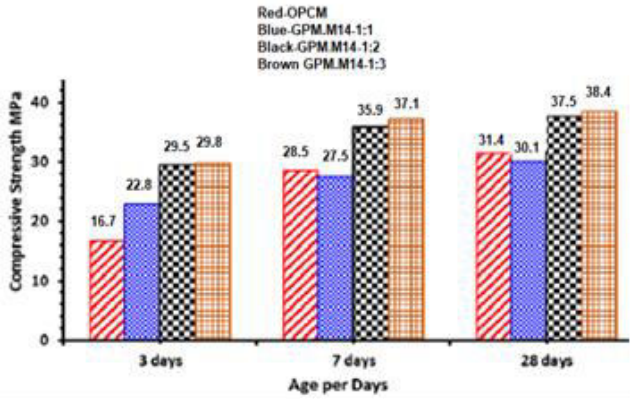

Figure-10. Effect of sodium silicate solution-to-sodium hydroxide solution with molarity M14 on compressive strength (for days: 3, 7 and 28).

Figure-11 shows the highest values of compressive strength in the case of molarity sixteen. This is because, at a high molarity of NaSi, the molecules are interacting in a faster way. This increases the complexity before NLGP thickens. NaSi has many types. The type used here is the Egyptian type.

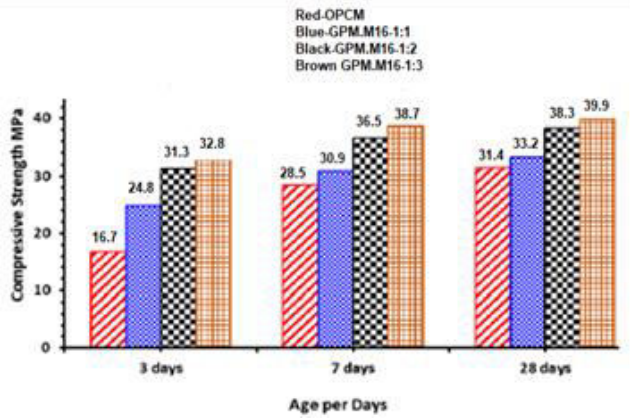

Figure-11. Effect of sodium silicate solution-to-sodium hydroxide solution with molarity M16 on compressive strength (for days: 3,7 and 28).

3.2.2 Final compressive strength with various NL concentrations %

The same mixing process of NLGP components was repeated with different concentrations of NL (0%, 1%, 3%, 6%, and 12%). The final results of compressive strength after 12 hrs, 3,7, and 28 days are shown in table-11 and Figures (12,13,14 and 15).

Table-11. The final results of compressive strength after 12 hrs, 3,7 and 28 days for (0%, 1%, 3%, 6% and 12%) NLGP.

Conc.	Comp. STr @ 12 hrs Mpa	Comp. STr @ 3 days MPa	Comp. STr @ 7 days MPa	Comp. STr @ 28 days MPa
0%	24	25.2	26.3	26.7
1%	25.8	27.1	29	30.1
3%	28.2	29.8	33.1	34.8
6%	39.6	41	44.9	47
12%	43.5	45	49.6	53.2 (7714 psi)

The results are shown in the mentioned figure in the same order to show the effect of increasing NL%. Colunm technique was used because it shows the comparison between results easily.

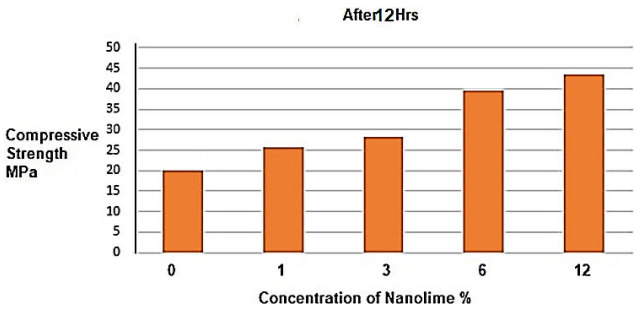

Figure-12. compressive strength after 12 hrs for (0%, 1%, 3%, 6% and 12%) NLGP.

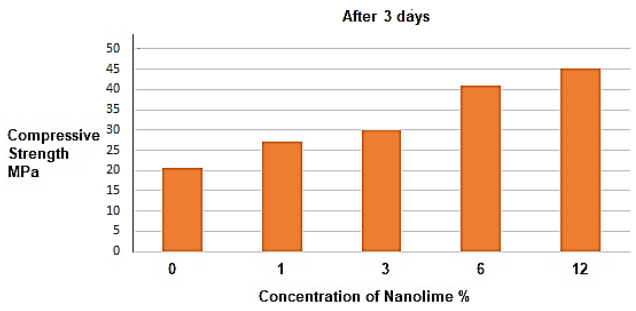

Figure-13. compressive strength after 3 days for (0%, 1%, 3%, 6% and 12%) NLGP.

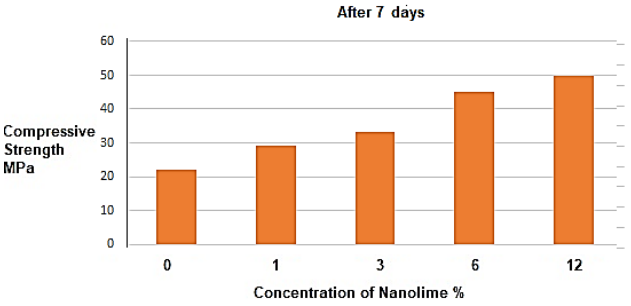

Figure-14. Compressive strength after 7 days for (0%, 1%, 3%, 6% and 12%) NLGP.

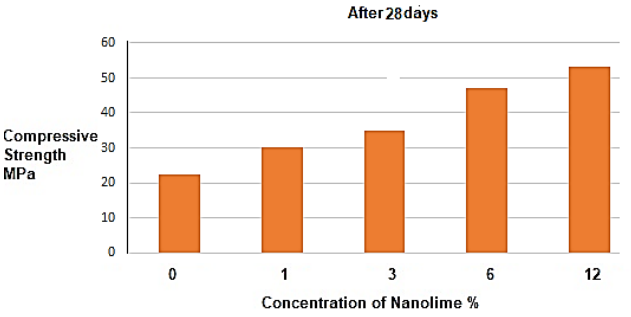

Figure-15. Compressive strength after 28 days for (0%, 1%, 3%, 6% and 12%) NLGP.

3.3 Skin factor

When NLGP is used a minimum damage to the formation is caused because the time of thickening and free water are controlled (Figure-16).

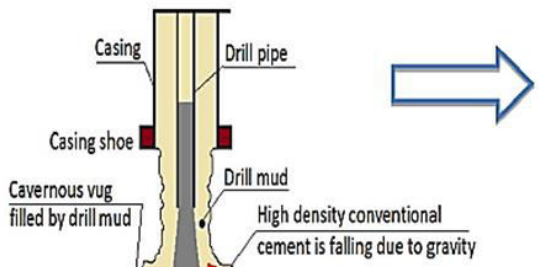

Figure-16. formation damage direction due to NLGP.

The formula of the skin factor is calculated as follows:

$$S = \frac{2\pi \cdot KH}{q\beta\mu} \Delta p_{skin} \quad \text{.....[Eq 3.11]}$$

Where

b.

K I s the formation permeability
H is the formation height
q is the flow rate of the fluid inside the skinned zone
B is the gas formation factor
μ is the fluid viscosity
▲P is the pressure difference across the skinned area

Flow rate can be calculated as:

2π R H L/t .....[Eq 3.12]

So the formula becomes

S = K t ▲P / R L .....[Eq 3.13]

Where

K is the permeability in (Darcy).
t is the time which is described as the maximum thickening time in (hrs).
▲P is the pressure difference = the reservoir pressure - the BWF in the bottomhole.
R is the hole radius (in).
L is the invasion depth which is obtained from the logs

The estimated volume of loss is 2 % of the volume of cement exposed to the formation
(0.04 π R H W_{ann})

c.
So the estimated length of invasion =
0.04 π R H W_{ann} / 2 π R H = 0.02 W_{ann} = 0.02 (Do-Di)..[Eq 3.14]

S = K t (P_{res}-P_{WF}) / 0.02 Do (Do-Di) .....[Eq 3.15]

d. The skin factor (S) is an indication of the damage inside the pay zone. In the case of using NLGP as cement for gas wells, S has a minimum value because thickening time (t) and pressure draw down (P_{res}-P_{wf}) are reduced.

NLGP was silled on the surface of both carbonate and shale rocks. Then a fluid pressure was applied to remove the NLGP from the surface of both the carbonate and shale rocks. NLGP needed a pressure equal to 40,000 psi to be removed from the carbonate rock surface and 20,000 psi to be removed from the shale rock surface (Figure-17).

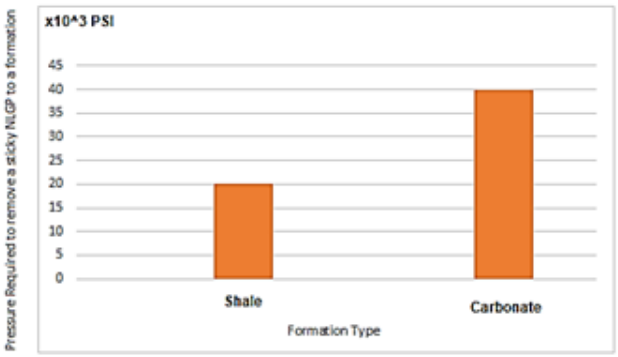

Figure-17. Pressure required to remove NLGP from the surface of carbonate and shale rocks.

4. DISCUSSIONS

4.1 Compressive Strength

4.1.1 Experimental results

After measuring the compressive strength value on the 3rd, 7th, and 28th days, data were represented in Figures: 1, 2, and 3. The results show that when the ratio between NaSi: NaOH is 1:3 (M16), the resulting compressive strength (on the 28th day) is higher than the ratios 1:1 by 20% and 1:2 by 4.2% (keeping the same M16). Also, as the molarity increases from M10 to M14 and then to M16, the resulting value also increases.

Although fly ash is very cheap as waste material and the final product (NLGP) is economical compared to Portland cement, the resulting compressive strength is high and sufficient for holding the casing and preventing gas channeling from high pressure zones up to 7500 psi. All the resulting compressive strength values in this research will be higher in the actual case. The reason is that the wellbore temperature will be higher, so the chemical reactions get quicker and more complex which will result in a more complex and stronger structure. The interpretation is that the particles of fly ash and NaSi liquid get more connected by NL and more activated by NaOH which makes polymerization more complex. The final mode of packing will be more compact because NL will exist among and be neatly packed to the bigger size particles. Therefore, the expectations of the product's performance is higher in an actual situation than the proposed one in this research.

It is clear that the value of compressive strength increases with time. The addition of NL resulted in a noticeable increase in the value of compressive strength especially in higher concentrations (6%, 12 %). Although the 1 and 3 % of NL resulted in compressive strength values with minimal differences, the gap between compressive strength values for 3 and 6% of NL is higher. In addition, 6 and 12 % of NL resulted in approximately closer values of compressive strength.

Similarly, the resulting values of compressive strengths in 12 hours and 3 days are closer to each other. But, there was a higher gap between compressive strength in the 3rd and the 7th days. However, the resulting values of compressive strengths in 7 and 28 days are approximately closer in value. This means that the economic product with optimum average compressive strength is obtained by a 6 % concentration of NL. In poor cement jobs, the most applicable product for solving gas channeling problem is 12% NLGP. It uses the highest concentration (12 %) of NL in order to reach a compressive strength value of 43.5 Mpa within 12 hours.

The results showed that all the values of compressive strength were obtained after exposing the samples to 60 degrees Celsius for 2 hours. If the temperature increases it means that higher values are obtained. The 12 % NLGP was exposed to 90 degrees celsius, the resulting compressive strength was 45.3 Mpa within 12 hours. This is greater than 43.5 Mpa in the case of 60 degrees Celsius. Consequently, for higher temperature formations, higher values of NLGP's compressive strength will be obtained. Therefore, in the case of poor cement jobs, a gas channeling problem is easier and quicker to be solved in high temperatures rather than the low temperature formation. Likewise, in deep water horizon, the formation temperature was 90 degrees Ceclius which means that NLGP would be a promising solution for that gas channeling problem.

In the case of using NLGP, the thickening time is more controlled which results in a reduction in the fluid losses inside the formation. So, NLGP reduces the formation damage. In addition, NLGP proved to be more adherent to various rock types. It needed a pressure equal to 40,000 psi to be removed from a carbonate rock and a pressure equal to 20,000 psi to be removed from a shale rock. Consequently, the formation type affects the adherence of NLGP to it. The stiffer the formation, the stronger the adherence of NLGP to it and the higher the required pressure to remove NLGP from it.

4.1.2 Comparison to cement fly ash (CF)

NLGP will be compared to CF which is a product mix between fly ash and cement. For clarity, CF product is more expensive than NLGP because the percentage of cement ranges from 30% to 70%. Consequently, NLGP is economically preferred rather than CF. Also in case of high temperatures (150° Celsius), NLGP will result in higher compressive strength values because the chemical reaction will be more motivated and complex for polymerization. Thus, when the results of CF at 150° Celsius are compared to NLGP at 60° Celsius, this means that the comparison is in favor of NLGP. Finally, the chosen NLGP's concentrations for comparison are 1%, 3% and 6% instead of 3%, 6% and 12%. This is in order to make the comparison in favor of NLGP to show the stronger effect of adding NL.

The comparison on the 28th day goes in three levels (Table-12). In the first level, 1% NLGP is compared with 70:30 cement to fly ash ratio. In the second level, NLGP with a concentration of 3% NL is compared with CF containing the same percent of cement and fly ash. In the third level, 6 % NLGP is compared with a 30:70 cement to fly ash ratio.

Table-12. Comparison between NLGP and CF.

Comparison levels in MPa	NLGP	CF
First Level	30.1	22
Second Level	34.8	28
Third Level	47	33

For the three levels, the ratios between the compressive strengths of NLGP to CF are 1.36, 1.24, and 1.42 respectively. This means that the compressive strength of NLGP is an average of 1.34 times the compressive strength of CF. Consequently, NLGP is more economical and practical than CF.

4.2 Case Study

In the deep water horizon (Figure-18), cement foam was used to reduce the losses to a low-pressure zone "pay zone". This method of loss control was used but without an optimum adjustment for the cement density. So, this resulted in an excessive reduction in cement hydrostatic pressure lower than the formation pressure. Consequently, hydrocarbons could channel to the surface and cause a blow-out (lost 11 billion dollars and 7 people died).

Figure-18. Deep water horizon incident (blow-out) in 2010.

In this incident, the required optimum value of cement density had to be designed accurately by nanotechnology. Obtaining such accurate density normally results in a precise hydrostatic pressure which is controlling formation pressure without causing neither mud losses nor formation damage. Optimum cement density can be obtained easily by NLGP, especially in critical situations like Deep water horizon. The other factor that can help in such a situation is the thickening time control. NLGP's thickening speed is controlled by designing the components to thicken at a specific temperature. Once NLGP is exposed to the designed formation temperature, it thickens faster than any kind of well cement (within 2 hours). NL % has an inverse relation to the required temperature of thickening. 12 % NL is recommended as the optimum concentration for NLGP's thickness within 2 hours at 90 ^{o}C (deep water horizon formation). However, if the trouble formation's temperature is above 90 ^{o}C, it is easier to control the problem within two hours with a 6 % NL. Consequently, the lost circulation problem is easier to solve at HPHT reservoirs and deep reach wells. In these wells, thickening should not happen before reaching the formation. Therefore, 12% NL is recommended for use in order to guarantee an accurate thickening response of NLGP because the molecules are in the neatest mode of packing which is required for thickening at a specific temperature (not lower nor higher).

For the criticality and importance of this case study a computer model is designed to help in making the calculations and making decisions faster because of the bigger volume of data (figure-19). In this figure if the skin factor is less than -5 or more than 5, the probability of NLGP loss or gas channeling increases respectively.

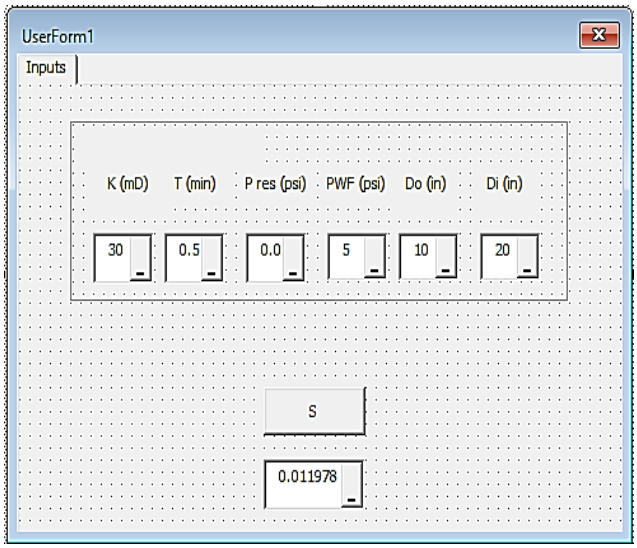

Figure-19. Model interface for skin factor calculations in case of using NLGP.

4.3 Profit Study

Higher molarity values result in higher compressive strength (Figures 9, 10, 11). But, using more chemicals increases the price. NL helped to get higher compressive strength values and more than the higher molarity ones. Therefore it is more economical.

The profit study (as per the experience of the chairman of Egypt Rock Mining company) will start with a building cement comparison The following is an economic comparison between NLGP's ton price and API cement for gas wells (class G) (minimum export price for the best quality cement)

The average ton price of NLGP (for average strength = 40-43 MPa) is calculated as follows (market prices in USD for May 2023):

Ton price of local NaOH = 10 X CC …...……....[Eq 3.1]
= 10 X 12.5
= 125 USD
0.10 per ton = 12.5 USD

Ton price oflocal NaSi = 5 X CC …....…..…....[Eq 3.2]
= 5 X 12.5
= 62.5 USD
0.05 per ton = 3.125 USD

Where CC is the ton price of calcium carbonate (60 micron size) = 12.5 USD

Price of solid components = ton price of (manufactured (non-waste))
fly ash + Ton of NL 6 % ……[Eq 3.3]

= CC + CC X 2 (nano process) X 0.06
= 1.12 X CC ……[Eq 3.4]
= 14 USD

0.85 per ton = 11.9 USD
Total cost = Ton price of NaOH + Ton price of NaSi + Price of solid components ……...…….[Eq 3.5]

= 12.5 + 3.125 + 11.9
= 27.525 USD

The manufacturing cost is around 12.5 USD per ton for mixing and grinding components of NLGP. Therefore, the final price is (40 USD).

Note that: Such processes do not need complex manufacturing machines (just mixing and grinding and no need for furnaces like cement needs).

Current price of local building cement = 125 USD /ton (May 2023)). Consequently, if NLGP is sold as a competitive product with top price = 120 USD /ton, the profit is 120 / 40 = (300 %).

For gas wells, NLGP is compared to Class G good quality cement for gas wells as follows:

The average ton price of NLGP (for average strength = 50-53 MPa) is calculated as follows (market prices in USD for May 2023) (the best quality of manufacturing components):

Ton price of imported NaOH = 30 X CC ……....[Eq 3.6]
= 30 X 17.5
= 525 USD
0.1 per ton = 52.5 USD
Ton price of imported NaSi = 15 X CC …...…..[Eq 3.7]
= 15 X 17.5
= 262.5 USD
0.05 per ton = 13.125 USD
Where CC is the ton price of calcium carbonate (32 micron size) = 17.5 USD
Price of solid components = ton price of fly ash (imported well ground best quality) + Ton of NL 6 % …..[Eq 3.8]
= 5 X CC + 2 X CC (nano process) X 0.12
= 5.24 X CC ……..…….[Eq 3.9]
= 5.24 X 17.5
= 91.7 USD
0.85 per ton = 78 USD
Total cost = Ton price of NaOH + Ton price of NaSi + Price of solid components ……..…….[Eq 3.10]
= 52.5 + 13.125 + 78
= 143.625 USD

The manufacturing cost is around 250 USD per ton for mixing and grinding components of NLGP in higher rpm and time for ensuring good quality using higher quality machines. Therefore, the final price is (394 USD).

Adding 100 USD for corrsion and H2S inhibitors per ton. Finally, the final price is (494 USD).

Current price of gas-wells API class G cement = 2000 USD /ton (minimum export price) (May 2023)). Consequently, if NLGP is sold as a competitive product with a top price = 1800 USD, the profit is 1800 / 494 = 365 %.

5. CONCLUSIONS

- NL is prepared experimentally by grinding and quenching calcium carbonate material.
- The nano-size distribution is measured by a dynamic light scattering device.
- NLGP product is cheaper than cement. It uses fly ash and limestone which are the main components. These two components are very cheap
- In NLGP, as the ratio between NaSi: NaOH increases, the resulting compressive strength increases (keeping molarity constant).
- When the molarity value increases, the resulting compressive strength increases. Compressive strength values increase with time and NL conc. %.
- The resulting values of compressive strength after 12 hours and on the 3rd day are closer to each other. Also, the compressive strength on the 7th and 28th days are closer to each other. But, there is a great gap between the compressive strength on the 3rd and the 28th days.
- The highest concentration 12 % of NL was used to reach a compressive strength = 43.5 Mpa within 12 hours. This value increased to 44.3 Mpa at 90 degrees Celsius.
- The controlled thickening time helps to reduce the formation damage.
- The skin factor in the case of NLGP is reduced because the thickening time and pressure draw down are so low.
- The stiffer the formation, the higher the required pressure to remove NLGP from it.
- In deep water horizon, the formation temperature was higher which means that NLGP is a promising solution for that hydrocarbon channeling.
- Faster thickening and higher compressive strength are obtained by 12% NLGP and higher formation temperature.

6. RECOMMENDATIONS

The samples were not left in water like concrete which would bring more strength. Also, the resulting compressive strength values were obtained without using gravel like concrete (which would cause higher compressive strength). The results showed that all the values of compressive strength were obtained after exposing the samples to 60 degrees Celsius for 2 hours. If

the temperature increases and exposure time increases, this means that higher values would be obtained.

7. INDEX

NLGP is nanolime-geopolymer
NL is nanolime
K is the formation permeability
H is the formation height
q is the flow rate of the fluid inside the skinned zone
B is the gas formation factor
μ is the fluid viscosity
▲P is the pressure difference across the skinned area
K is the permeability in (Darcy).
t is the time which is described as the maximum thickening time in (hrs).
▲P is the pressure draw down = $P_{res} - P_{wf}$
P_{res} is the reservoir pressure
P_{wf} is the bottom-hole flowing pressure
R is the bottom-hole radius (in).
L is the invasion depth which is obtained from the logs
S is the skin factor
HPHT is the high pressure high temperature formation
M is the molarity of NaSi

The data that support the findings of this study are available from the corresponding author, [Mario E. S. Abdelmalek, upon reasonable request.

REFERENCES

[1] Mohamed Alkhamis, Abdulmohsin Imqam, Missouri Univ. of Science & technology. 2018. New Cement Formulations Utilizing Graphene Nano Platelets to Improve Cement Properties and Long-term Reliability in Oil Wells. SPE Paper-192342-MS, SPE Technical Symposium & Exhibition, Dammam, Saudi Arabia.

[2] Shawgi Ahmed, Chinedum Peter E., Saeed Salehi. 2018. Improvement in Cement Sealing Properties & Integrity Using Conductive Carbon Nano Materials: From Strength to Thikening Tim. SPE Paper-191709-MS, SPE Annual Technical Conference & Exhibition, Dallas, Texas, USA.

[3] Maryam Tabatabaei, Arash Dahi Talehgani, Nasim Alem, Pennsylvania State University. 2019. Economic Nano-Additive to Improve Cement leaking Capacity. SPE Paper-195259-MS, SPE Western Regional Meeting, San Rose, California, USA.

[4] Mobeen Murtaza, Mohamed Mahmoud, Salaheldin Elkatatny, Abdulaziz Al Majed, Weiqing Chen, and Abul Jamaluddin, King Fahd University of Petroleum & Minerals. 2019. Experimental Investigation of the Impact of Modified Nano Clay on the Rheology of Oil Well Cement Slurry. SPE Paper-19456-MS, SPE International Petroleum Technology Conference, Beijing, China.

[5] Haichuan Lu, Huikai Zheng, Zongyao Li, Wangsheng Feng and Shaobing Tang, Jianlong Zou, Lirong Li and Wenli Tan. 2019. Key Laboratory of Drilling Engineering of CNPC. 2019. The Study and Application of Intelligent Thixotropic Cement Slurry Based on Nanotechnology. SPE Paper-19148-MS, SPE International Petroleum Technology Conference, Beijing, China.

[6] R. de. La Roije C. Egyd. 2012. Nano-Engineered Oil Well Cement Improves Flexibility and Increases Compressive Strength, A Laboratory Study. SPE Paper-156501, SPE International Petroleum Technology Conference, Noordwijk, Netherkands.

[7] Maryam T. Arash D. 2019. Economic Nan-Additive to Improve Cement Sealing Capacity. SPE Paper-195259-MS, SPE Western Regional Meeting, San Jose, California, USA.

[8] Vip C., Amani N. 2015. Behavior of Nano Calcium Carbonate Modified With Smart Cement Contaminated With Oil Based Drilling Mud. OTC-25845, SPE Offshore Technology Conference, Texas, USA.

[9] Amin A. Tyler C., Geir H. 2017. Barite Nanoparticles Reduces The Cement Fluid Loss. SPE-185114-MS, Oil and Gas Symposium, Oklahoma, USA.

[10] Chimaroke A. Momoh M. 2016. University of Port Harcourt: Experimental Evaluation of Particle Sizing in Drilling Fluid to Minimize Filtrate Losses and Formation Damage. SPE-184303-MS, SPE Annual International Conference, Nigeria.

[11] Mario A. mahmoud T., Shady R. 2022. Using Nanotechnology for Enhancing Cement Properties in Gas Wells. IJEAIS (IJAAR) ISSN: 2643-9603, 6(4).

[12] Aiken T. A., Kwasny J., Sha W., *et al.* 2018. Effect of slag content and activator dosage on the resistance of fly ash geopolymer binders to sulfuric acid attack. Cement and Concrete Research. 111, 23e40.

[13] Aliques-Granero J., Tognonvi M. T., Tagnit-Hamou A. 2019. Durability study of AAMs: sulfate attack resistance. Construction and Building Materials 229, 117100.

[14] Lahoti M. K., Tan K. H., Yang E. H. 2019. A critical review of geopolymer properties for structural fire-resistance applications. Construction and Building Materials. 221, 514e526.

[15] Liu J., Hu L., Tang L., *et al*. 2020b. Utilisation of municipal solid waste incinerator (MSWI) fly ash with metakaolin for preparation of alkali-activated cementitious material. Journal of Hazardous Materials. 402, 123451.

[16] Liu Y., Su P., Li M., *et al*. 2020c. Review on evolution and evaluation of asphalt pavement structures and materials. Journal of Traffic and Transportation Engineering (English Edition). 7(5): 573e599.

[17] Shill S. K., Al-Deen S., Ashraf M., *et al*. 2020. Resistance of fly ash based geopolymer mortar to both chemicals and high thermal cycles simultaneously. Construction and Building Materials. 239, 117886.

[18] Abdel-Ghani N. T., Elsayed H. A., AbdelMoied S. 2019. Geopolymer synthesis by the alkali-activation of blastfurnace steel slag and its fire-resistance. HBRC Journal. 14(2): 159e164.

[19] Lyu X., Wang K., He Y., *et al*. 2019. A green drying powder inorganic coating based on geopolymer technology. Construction and Building Materials. 214, 441e448.

[20] Wang K., Tang Q., Cui X., *et al*. 2016. Development of near-zero water consumption cement materials via the geopolymerization of tektites and its implication for lunar construction. Scientific Reports. 6, 29659.

[21] Dindi A., Quang D. V., Vega L. F., *et al*. 2019. Applications of fly ash for CO2 capture, utilization, and storage. Journal of CO2 Utilization. 29, 82e102.

[22] Li Y., Min X., Ke Y., *et al*. 2018. Utilization of red mud and Pb/Zn smelter waste for the synthesis of a red mud-based cementitious material. Journal of Hazardous Materials. 344, 343e349.

[23] Yang Z., Mocadlo R., Zhao M., *et al*. 2019. Preparation of a geopolymer from red mud slurry and class F fly ash and its behavior at elevated temperatures. Construction and Building Materials. 221, 308e317.

[24] Zhang J., Zhang S., Liu B. 2020d. Degradation technologies and mechanisms of dioxins in municipal solid waste incineration fly ash: a review. Journal of Cleaner Production. 250, 119507.

[25] Zhao Y., Liang N., Chen H., *et al*. 2020. Preparation and properties of sintering red mud unburned road brick using orthogonal experiments. Construction and Building Materials. 238, 117739.

[26] Peiliang C., Yaqian C. 2014. Advances in geopolymer materials: A comprehensive review. 283e314.

[27] Renggugang L., Yijin Z., Shiming Z., Peiqing L., Kui L. 2022. Compressive Strength and Hydration Products of Oil Well Cement Mixed with Fly Ash at Ultra-high Temperature. Journal of advanced concrete technology. 20: 484-491.